ELSEVIER

Ceramics International 28 (2002) 59–67

CERAMICS INTERNATIONAL

www.elsevier.com/locate/ceramint

The use of Saudi slag for the production of glass-ceramic materials

G.A. Khater*,[1]

Glass Research Department, National Research Center, Dokki, Cairo, Egypt

Received 12 December 2000; received in revised form 1 January 2001; accepted 22 April 2001

Abstract

Uniform, ultrafine, microcrystalline, glass-ceramic materials have been obtained successfully from silicon manganese slag and steel slag. The silicon manganese slag reached was about 90 wt.% and steel slag reached was about 57 wt.% of the batch constituents. Depending on the composition, batches were melted in the range of 1200–1300 °C. The glass obtained and the corresponding heat treated specimens were examined by DTA, X-ray diffraction and polarizing microscope. It has been found that increasing the content of the bustamite phase in the glasses, results in an increased bulk crystallinity when treated at 1000 °C/2 h. On the contrary, an increase in the content of fayalite phase in the glasses results in decreased bulk crystallinity when treated at 1000 °C/2 h.

Keywords: Slag-glass; Crystallization; Diopside; Anorthite; Bustamite

1. Introduction

"Slag" is the general term applied to the residue drawn off in the process of refining a metal from ore. Sometimes discarded, it is more often utilized because of its physical characteristics, such as for road stone, railroad ballast, building blocks, cement etc. The chemical composition of this vitrified glass-like residue of the blast furnace is very much like that of glass—and from this "by-product" is produced the material called "Calcumite" slag.

It was generally known that the use of slag as a new material in the batch could increase the efficiency of the glassmaking process. But since it is a by-product, iron and steel producers do not emphasize control of the chemical variations of slag, except as it might affect their basic iron product, and consequently, the primary drawback to the general use of this unprocessed material in glassmaking is the difficulty in controlling chemical variations.

Because glass and glass ceramics are known to have many commercial applications, the transformation of waste into glass or glass-ceramics provides the opportunity for making useful, marketable products out of waste, even hazardous wastes. In fact this is already being done throughout the United States. For example, Oregon Steel Mills transformed their hazardous electric arc furnace dust into glass granules and sold them as grit blasting sand or grit for asphalt roofing shingles. Glass frit made by quenching the molten glass in water forms small sharp edged particles with a size ranging from 0.02″ to 0.12″. This product can be made from almost any typical waste stream.

More than 12 million m^3 (1982) of slag-glass ceramic is produced and exploited and economic efficiency of its introduction into industry in place of conventional materials has exceeded one million USD. Also approximately 18 million m^3 of slag per year are produced by the iron and steel industry in the United States. In Saudi Arabia approximately 350 thousand m^3 (1999) of slag per year are produced by steel industry and more than 70 thousand m^3 of silicon manganese slag are produced by alloys industry.

The use of waste materials such as silicon manganese slag, steel slag, blast-furnace slag and pass cement dust for the production of glass-ceramic materials is of great economic technological and scientific importance with proper correction of the chemical composition.

The different types of slags can be used successfully for the production of crystalline-glass materials of different microstructures and mineralogical constitutions that have many valuable technical properties. The nature and character of the crystalline phases and the microstructure of the materials are the most important factors affecting the technical properties of the glass ceramics [1–3].

* Tel.: +9661-478-0000x22; fax: +9661-476-3875.
E-mail address: gamal@awalnet.net.sa
[1] Corresponding address: PO Box 609, Riyadh 11421, Kingdom of Saudi Arabia.

0272-8842/02/$22.00
PII: S0272-8842(01)00058-X

Extensive investigation has been carried out dealing with the crystallization of the glasses and/or melts based on natural rocks and waste of materials under ordinary pressure during trials to obtain new crystalline glass materials (glass-ceramics) from cheap resources.

Glass-ceramics are used in a wide range of technical applications, for example, in construction and for domestic purposes and in the microelectronics industry [4].

Locsei [5] could obtain glass-ceramic materials characterized by high wear resistance and chemical durability from glasses based on blast furnace slags, sand and clay with some additions of crystallization catalyst.

Zhunina et al. [6] studied the crystallization of glasses based on fusible calcareous clays. They obtained crystalline materials composed mainly of pyroxene. They found that Cr_2O_3 and TiO_2 were the most effective crystalline catalysts.

Omar and Salman [7] studied the crystallization process of molten granite and dolomite mixtures. Materials composed of alkali aluminous pyroxene, melilite and olivine assemblages were obtained.

Khater [8] managed to obtain a glass-ceramic material characterized by low thermal expansion coefficient from glasses based on Egyptian clay, sand, $MgCO_3$ and Li_2CO_3 with some additions of crystalline catalyst.

Khater [9] synthesized basalt melt cast ceramic materials composed of monomineralic pyroxene. The outstanding strength, the excellent abrasion and chemical resistance are the most valuable features of these materials.

El-Shenawi et al. [10] studied the crystallization of monopyroxenic basalt-based glass-ceramic. They obtained crystalline materials composed of pyroxene. The principal proposed usage for basalt and slag derived glass ceramics is in the form of tiles and pipes for the conveyance or storage of abrasive materials where the glass ceramics are much more resistant to abrasion than alternative metals and alloys. Although only limited work has been carried out in the UK and USA [11,12], a great deal of development and use has been undertaken in Russia [13]. It is an indication of its value that is claimed that this application may represent the greatest use of glass ceramics worldwide.

The aim of this paper is to use the waste materials such as silicon manganese slag and steel slag with other additives for the production of glass-ceramic materials which are of great economic technological and scientific importance with proper correction of the chemical composition.

2. Experimental procedure

2.1. Design of glass compositions and batch preparation

The present work involved two series of slag which were studied (i) silicon manganese slag from Sabayek Company, Saudi Arabia, (ii) steel slag from Hadeed Company, Saudi Arabia. Table 1 presents the chemical composition of the materials used for batch preparation, while Tables 2 and 3 present the nominal compositions were formulated via modification of the normative slag composition

(i) Silicon manganese slag "series 1". Five glass compositions within the bustamite $CaMn(SiO_3)_2$–diopside ($CaMgSi_2O_6$) + anorthite ($CaAl_2Si_2O_8$) system were selected for the present work. These compositions are based on the diopside (58 wt.%) anorthite (42. wt.%) eutectic composition with successive additions of bustamite up to 50 wt.% at 10 wt.% intervals of the bustamite component. The compositions studied were designated G1, G2, G3, G4 and G5, were the number indicates the wt.% of the bustamite component and the rest being the diopside + anorthite components in their mutual eutectic ratio. The batches corresponding to these compositions were prepared by mixing the calculated appropriate proportions of silicon manganese slag, sand, limestone, clay and talc. Table 2 gives the details of glass compositions in oxide percentages and percentages of raw materials.

(ii) Steel slag "series 2" five glass compositions within the fayalite (Fe_2SiO_4)–diopside ($CaMgSi_2O_6$) + anorthite ($CaAl_2Si_2O_8$) system were selected for the present work. These compositions are based on the diopside (58 wt.%) anorthite (42 wt.%) eutectic composition with successive additions of fayalite up to 50 wt.% at 10 wt.% intervals of the fayalite component. The compositions studied were designated F1, F2, F3, F4 and F5; where the number indicates the wt.% of the fayalite component and the rest being the dipside + anorthite components in their mutual eutectic ratio.

The batches corresponding to these compositions were prepared by mixing the calculated appropriate proportions of steel slag, sand, clay, dolomite and limestone. Table 3 gives the details of glass compositions in oxide percentages and percentages of raw materials.

After being thoroughly mixed, the weighed powdered batch materials were melted in Pt. Crucibles in a globar furnace at temperatures ranging from 1200 to 1300 °C for 2–3 h depending upon composition; the melts. The homogeneity of the melt was achieved by swirling of the melt-containing crucible several times at about 20-min intervals. After melting and refining, the bubble-free melt was cast onto a hot steel marver into buttons and rods. The hot glass samples were then transferred to a pre-heated electric muffle furnace for annealing.

2.2. Thermal treatments

The effect of heat treatment on crystallization was studied in glass samples that had been cured isothermally at temperatures in the range of 900–1000 °C for 2 h (series 1) and at temperatures in the range of 800–950 °C for 2 h (series 2).

Table 1
Chemical composition of the raw material

Oxide (wt.%)	Silicon manganese slag	Steel slag	Limestone	Quartz sand	Clay	Dolomite	Talc
SiO_2	45.00	14.20	0.15	99.20	55.16	0.54	62.00
TiO_2	0.22	1.14	Nil	trace	1.89	0.40	–
Al_2O_3	9.00	8.12	0.22	0.28	28.31	0.50	1.60
Fe_2O_3	0.75	34.89	0.03	0.03	0.16	0.18	0.40
MgO	11.00	10.76	0.10	trace	0.18	20.95	30.30
CaO	22.00	24.48	55.70	0.10	0.34	30.90	0.40
Na_2O	trace	trace	trace	trace	0.30	trace	0.32
K_2O	trace	trace	trace	trace	0.20	trace	0.11
MnO	12.00	3.87	–	–	–	–	–
I.L.	–	–	43.80	0.40	10.46	46.90	4.7

Table 2
Chemical composition of the glasses (series 1)

Glass no.	Nominal phase composition (wt.%)			Calculated composition (wt.%)					Raw materials (wt.%)				
	Bust.	Di.	An.	SiO_2	Al_2O_2	CaO	MgO	MnO	Si Mn slag	Sand	Limestone	Clay	Talc
G10	10	52.20	37.80	50.18	13.87	23.42	9.67	2.87	19.50	3.18	27.10	31.28	18.94
G20	20	46.40	33.60	50.00	12.33	23.33	8.59	5.75	35.11	20.04	17.30	19.40	7.85
G30	30	40.60	29.40	49.82	10.79	23.25	7.52	8.62	65.65	8.94	12.46	12.95	–
G40	40	34.80	25.20	49.64	9.25	23.17	6.44	11.50	90.26	6.13	3.60	–	–
G50	50	29.00	21.00	49.47	7.71	23.09	5.37	14.37	75.00	14.27	10.72	–	–

Bust. = bustamite $CaMn(SiO_3)_2$; Di. = diopside ($CaMgSi_2O_6$); An. = anorthite ($CaAl_2Si_2O_8$), Si Mn Slag = silicon manganese slag.

Table 3
Chemical compostion of the glasses (series 2)

Glass no.	Nominal phase composition (wt.%)			Calculated composition (wt.%)					Raw materials (wt.%)				
	Fay.	Di.	An.	SlO_2	Al_2O_3	CaO	MgO	FeO	Steel slag	Sand	Clay	Dolomite	Limestone
F10	10	52.20	37.80	48.26	13.87	21.15	9.67	7.06	16.86	18.78	29.55	28.62	6.19
F20	20	46.40	33.60	46.16	12.33	18.80	8.59	14.12	35.59	21.61	22.49	15.62	4.69
F30	30	40.60	29.40	44.07	10.79	16.45	7.52	21.17	56.78	24.92	14.66	1.20	2.43
F40	40	34.80	25.20	41.97	9.25	14.10	6.44	28.23	65.46	29.90	4.65	–	–
F50	50	29.00	21.00	39.89	7.71	11.75	5.37	35.28	66.34	31.66	–	–	2.00

Fay. = fayalite (Fe_2SiO_4); Di. = diopside ($CaMgSi_2O_6$); An. = anorthite ($CaAl_2Si_2O_8$).

2.3. Differential thermal analysis (DTA)

Eighty milligrams of the powdered glass sample (<0.60–>0.25 min), a heating rate of 10 °C/min from room temperature to 1050 °C and sensitivity of 20 μV/inch were adopted through a Netzsch apparatus.

2.4. X-ray diffraction analysis (XRD)

Powder X-ray diffraction patterns were obtained using a Phillips X-ray diffractometer type PW 1050, adopting Ni-filtered Cu radiation, operated at 36 kV and 16 mA. All the instrument settings were maintained for all the analyses and an external standard, namely a silicon disc, was always used to test this maintenance.

2.5. Polarizing microscopy

The mineralogical constitution and microstructures of heat-treated samples were examined whenever possible in thin section using a polarizing Carl–Zeiss research microscope.

3. Results

3.1. Crystallization of glasses based on fayalite–diopside–anorthite system (series 1)

Differential thermal analysis of the glasses (Fig. 1) showed various endothermic effects. These small heat

absorptions may indicate the molecular rearrangement phenomenon preceding glass crystallization i.e. pre-crystallization stage [14]. Exothermic peaks indicating crystallization reaction are also recorded. As the bustamite content in the glass composition was increased the peak temperature of the crystallization exotherms decrease also the endothermic effects mentioned above were slightly displaced towards lower temperatures. These effects may be ascribed to the viscosity temperature relations of the glasses since the upward shift of the endotherms may indicate lower viscosities, which was noted during melting and casting.

Visual and petrographic investigation (Figs. 2–5) of the heat-treated glasses showed that crystallization

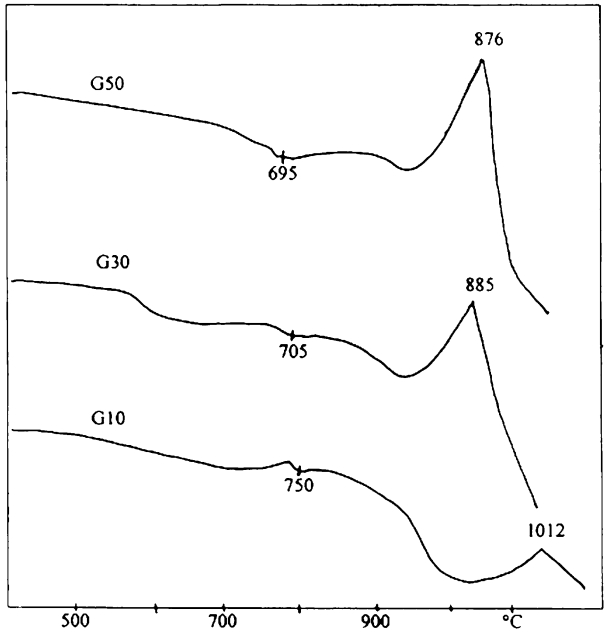

Fig. 1. Differential thermal analysis curves of glasses based on bustamite–diopside–anorthite system (series 1).

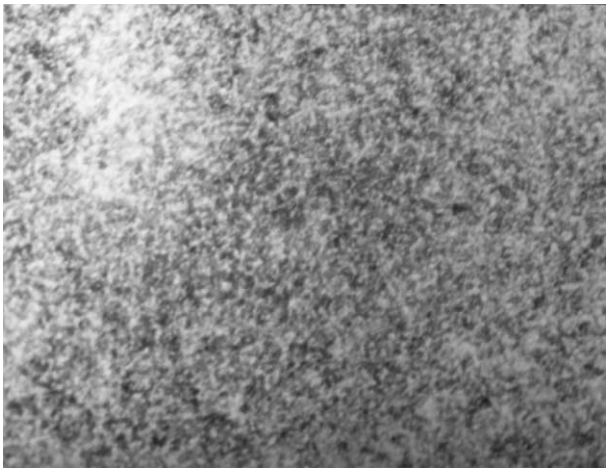

Fig. 2. G10 (1000 °C, 2 h). Fine grained holocrystalline mass of diopside, anorthirte and bustamite C.N., ×250.

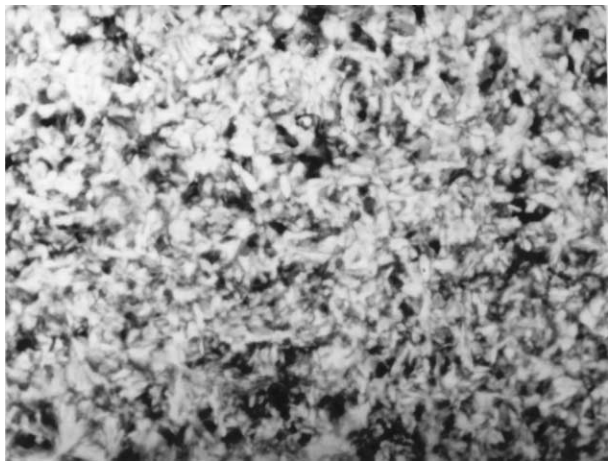

Fig. 3. G20 (1000 °C, 2 h). Minute irregular intergrowths of diopside, anorthite and bustamite ferroan C.N., ×250.

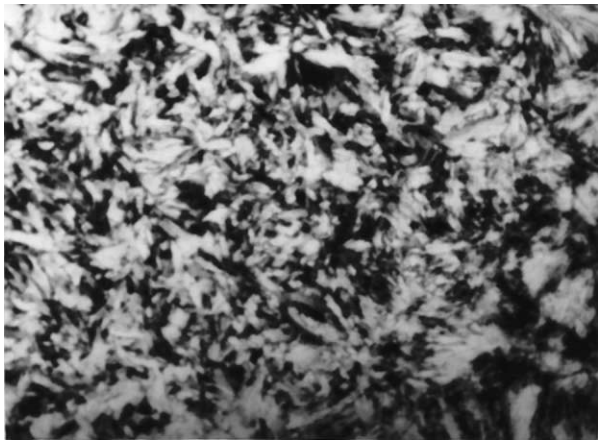

Fig. 4. G30 (1000 °C, 2 h). Holocrystalline mass of spheruthic diopside with fine anorthite microlites, short prismatic wollastonite with small equidimensional pyroxymangite C.N., ×250.

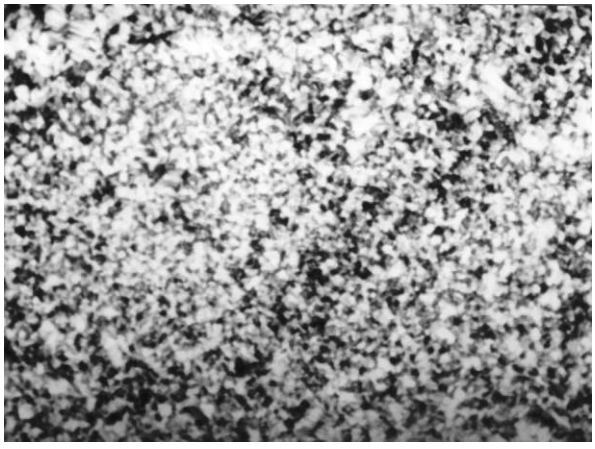

Fig. 5. G50 (1000 °C, 2 h). Fine-grained holocrystalline mass of diopside solid solution and bustamite ferroan C.N., ×100.

began G10 and G20 by surface nucleation and in the bustamite-rich glasses G30, G40 and G50 by both surface and bulk nucleation, with the latter predominating in G30 and G50, crystallization readily took place throughout the entire volume of these two glasses.

The above observations, therefore, indicate that an increase in the bustamite content in the glasses up to a certain limit, is desirable for enhancing the crystallizability of the glass through bulk nucleation and for lowering the temperature of the onset of crystallization which in turn favours the formation of undeformed crystalline products.

X-ray diffraction (Table 4 and Fig. 6) showed that diopside ($CaMgSi_2O_6$) or a diopsidic solid solution ($CaMgSi_2O_6.CaAl_2SiO_6$) anorthite ($CaAl_2Si_2O_8$), wollastonite ($CaSiO_3$), pyroxymangite ($MnSiO_3$) and bustamite (bustamite ferroan Ca(Mn, Fe) Si_2O_6 and bustamite calcian Ca(Mn, Ca)Si_2O_6 the main crystalline phases developed in the glases, their frequency depending on the composition (Fig. 6) depicts the X-ray diffraction

Table 4
Phases developed from thermally crystallized glasses based on the bustamite–diopside–anorthite system (series 1)

Glass no.	Heat-treatment	Phases developed
G10	1000 °C, 2 h	Diopside, anorthite, bustamite
G20	1000 °C, 2 h	Diopside, anorthite, bustamite, ferroan
G30	1000 °C, 2 h	Diopside, anorthite, wollastonite, pyroxymangite
G40	1000 °C, 2 h	Diopside ss, bustamite–calcian
G50	1000 °C, 2 h	Diopside ss, bustamite–ferroan

ss = Solid solution.

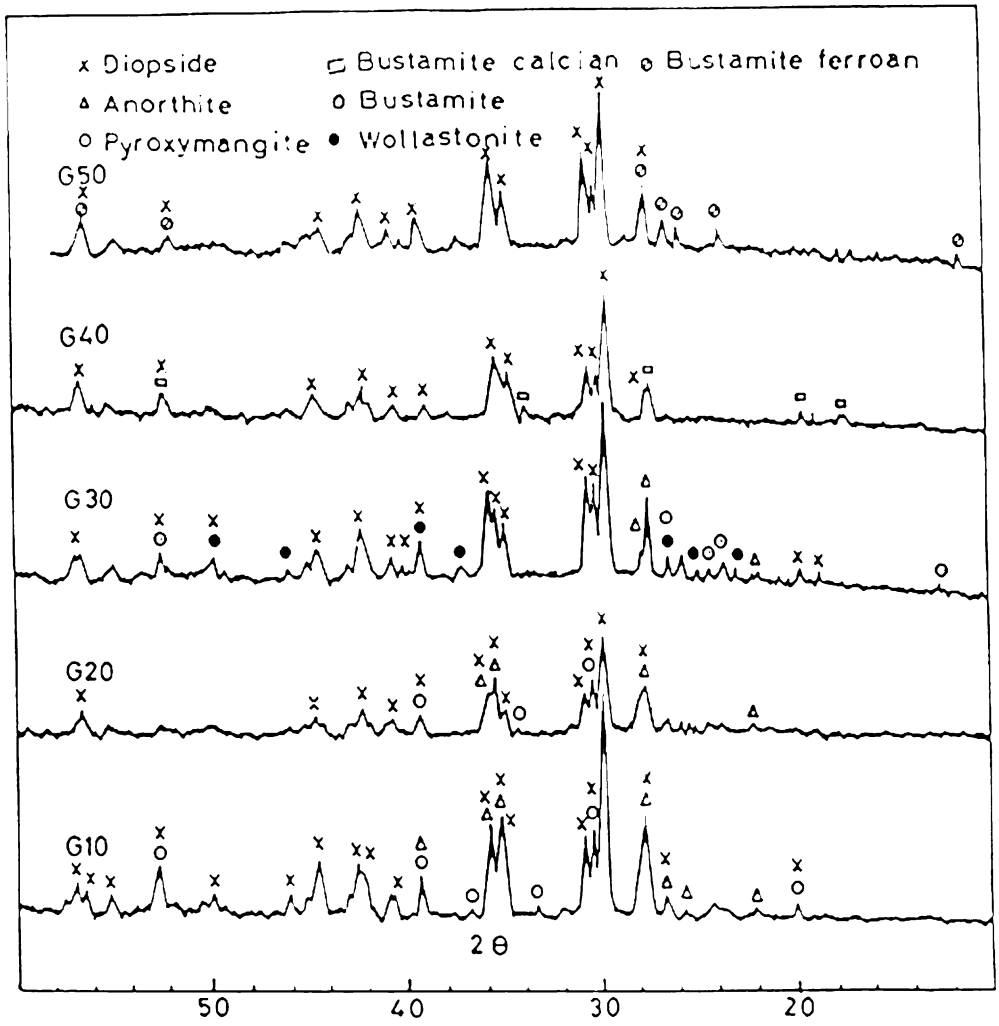

Fig. 6. X-ray diffraction patterns of glasses based on the bustamite–diopside–anorthite system heat-treated at 1000 °C for 2 h.

traces of glasses G10–G50 treated under the same conditions. Samples of G10 and G20 diopsidic pyroxene, anorthite and bustamite phases were formed (Fig. 6). Sample G30 diopsidic pyroxene as a major crystalline phase together with anorthite and bustamite transformed into wollastonite and pyroxymangite (Fig. 6). Samples of G40 and G50 diopsidic pyroxene as a major crystalline phase, anorthite disappeared and bustamite (calcian and ferroan) appeared (Fig. 6).

3.2. Crystallization of glasses based on fayalite–diopside–anorthite (series 2)

Differential thermal analysis of the glasses (Fig. 7) showed various endothermic effects. These small heat absorptions indicate phenomena preceding bulk glass crystallization, at this stage atoms began to arrange themselves in a preliminary structural element subsequent to crystallization. Exothermic peaks indicating crystallization reactions are also recorded. As the fayalite content in the glass composition was increased, the peak temperature of the crystallization exotherms decreases, also the endothrermic effects mentioned above were slightly displaced towards lower temperatures. These effects may be ascribed to the viscosity temperature relations of the glasses since the upward shift of the endortherms may indicates higher viscosities, which was noted during melting and casting.

Visual and petrographic investigation (Figs. 8–11) of glasses F10, F20 and F40 showed that they began to crystallize at approximately 800 °C showing volume crystallization to an almost holocrystalline mass without deformation during thermal treatment and in the fayalite-rich glasses F50 by both surface and bulk nucleation.

Table 5
Phases developed from thermally crystallized glasses based on the fayalite–diopside–anorthite system (series 2)

Glass no.	Heat-treatment	Phases developed
F10	1000 °C, 2 h	Augite
F20	1000 °C, 2 h	Augite
F30	1000 °C, 2 h	Diopside, anorthite, fayalite
F40	1000 °C, 2 h	Diopside–hedenbergite, anorthite, magnetite
F50	1000 °C, 2 h	Diopside–hedenbergite, anorthite, magnetite

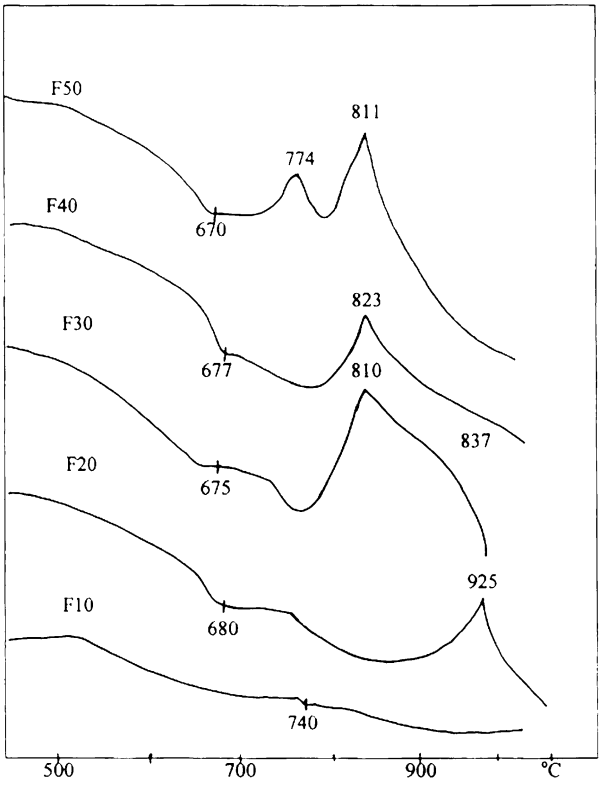

Fig. 7. Differential thermal analysis curves of glasses based on fayalite–diopside–anorthite system.

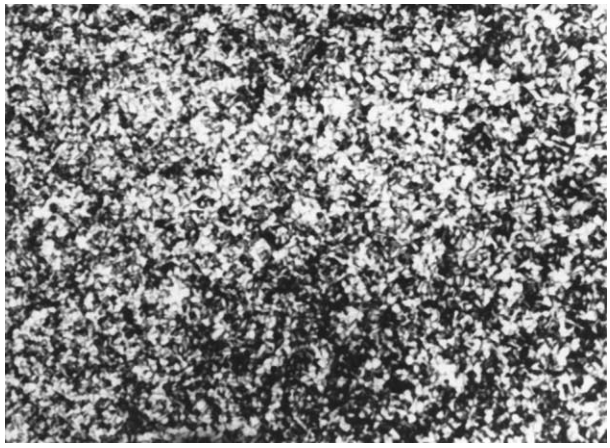

Fig. 8. F40 (1000 °C, 2 h). Volume crystallization of the aggregates of diopside–hedenbergite, anorthite and magnetite C.N., ×100.

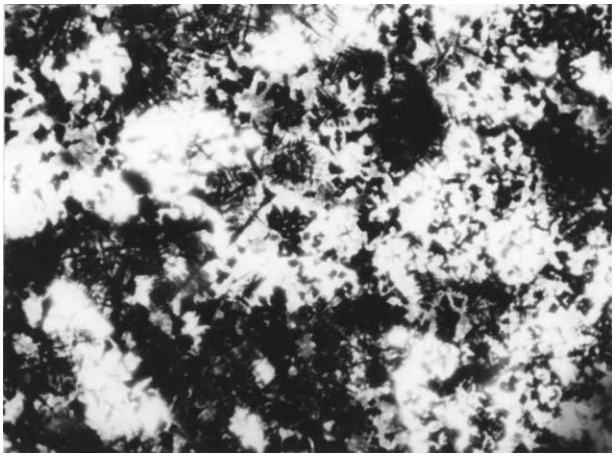

Fig. 9. F50 (1000 °C, 2 h). Fine intergrowths of diopside, anorthite and magnetite C.N., ×250.

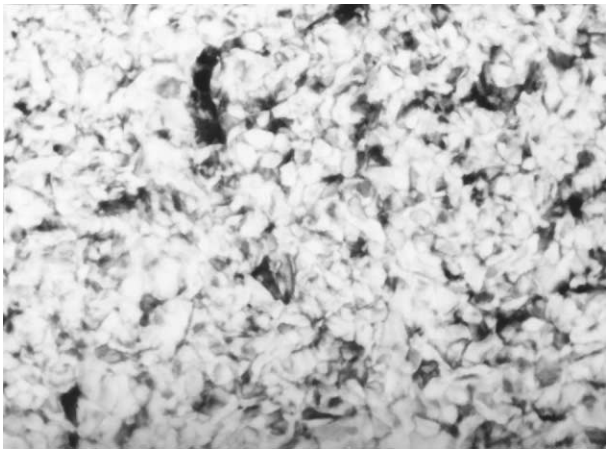

Fig. 10. F10 (1000 °C, 2 h). Volume crystallization aggregates of augite crystals C.N., ×250.

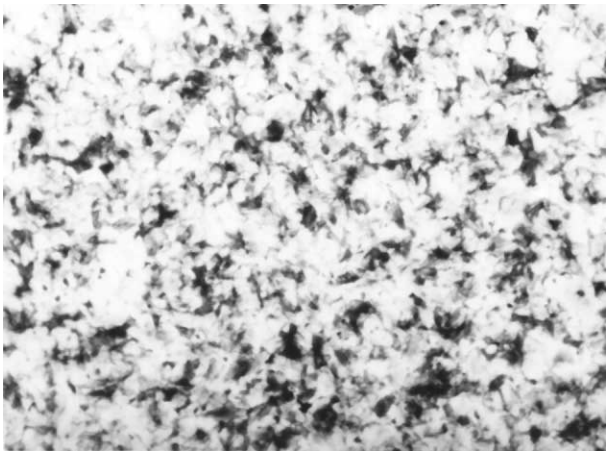

Fig. 11. F20 (1000 °C, 2 h). Similar to the above C.N., ×250.

The above observations, therefore, indicate that the decrease in the fayalite content in the glasses is desirable for enhancing the crystllizability of the glass through bulk nucleation and favours the formation of undeformed crystalline products.

Fig. (12) depicts the X-ray diffraction traces of samples F10–F50 treated under the same conditions. Samples F10 and F20 augite phase (Ca, Fe, Mg) SiO_3 (monomineralic phase) was formed (Fig. 12). For sample F30 diopsidic pyroxene ($CaMgSi_2O_6{\cdot}CaAl_2SiO_6$) was a major crystalline phase with appearance of anorthite ($CaAl_2Si_2O_8$) and fayalite (Fe_2SiO_4) phases (Fig. 12). For samples F40 and F50, the picture X-ray patterns become more explicit and magnetite (Fe_2O_3) appeared and the fayalite (Fe_2SiO_4) phase disappeared. An increase in the intensities and explicity the anorthite diffraction lines (e.g. anorthite lines 4.05, 3.66 and 3.29 Å) with consequent decrease of the intensities of diopside pattern. (e.g. 3.04, 2.91 and 2.54 Å) could be observed in Fig. 12.

4. Discussion

(i) Series No. 1: from the Bustamite–diopside–anorthite system (Figs. 2–5) it can be noticed that as the bustamite content (consequently MnO content) of the glass increases, the tendency of the glass to crystallize throughout the bulk increases. At about 50 wt.% the bustamite, sample G50, has a tendency towards bulk crystallization increasing sharply and it is, therefore, possible to relate such a high tendency towards bulk crystallization to the effect played by Mn^{2+} ions.

In typical complex glasses many workers [15–21] consider that the interfacial energy between two glassy phases is less than that between a glass and crystalline phase, thereby reducing the barrier to nucleation.

Mn^{2+} ions may be responsible for encouraging bulk crystallization on going from G10 to G 50 as a result of the possible change in its coordination from tetrahedral to octahedral. The coordination state of Mn^{2+} ions in silicate glasses has been the subject of considerable debate. With addition and increase of the bustamite content in glasses from G10 to G50 a corresponding decrease in the alkaline earth oxides occurs, accompanied by an increase in the MnO content (Table 2 in the direction from G10 to G50). Consequently the sharing of Mn^{2+} in fourfold coordination is expected to increase. This would enhance the formation of highly viscous regions causing phase separation that acts at nucleating centres. The present attribution explains the increased probability toward crystallization with an increase in the content of bustamite (Fig. 6).

With addition of bustamite on diopside–anorthite eutectis (G10 and G20) there was no significant effect on the phases formation (Fig. 6). In G30 bustamite transformed into wollastonite and pyroxymangite. A further increase in the bustamite content to 40–50 wt.% (G40 and G50) gives bustamite with diopside pyroxene and anorthite that disappeared from X-ray examination of heat-treatment at 1000 °C for 2 h. The results (Fig. 6) revealed that the amounts of diopside crystallized in these glasses are greater than their normative amounts. The diopside pyroxene seems to represent the major crystalline phase in the fully crystallized specimens. The high frequency of the diopside phase together with the noticed slightly higher 2θ values, relative to the standard ASTM d-spacing [22], indicates a considerable solid solution most probably of Ca-Tschermak's componet $CaAl_2SiO_6$ in diopside. The silica rest from anorthite enter in bustamite to form bustamite solid solution.

(ii) Series 2: from the Fayalite–diopside–anorthite system (Figs. 8–11) it can be noticed that the fayalite content (consequently FeO content) of the glass decreases. At about 20 wt.% fayalite (sample F20) the tendency towards bulk crystallization increases sharply and it is, therefore, possible to relate such a high tendency towards bulk crystallization to the effect played by Al^{3+} ions.

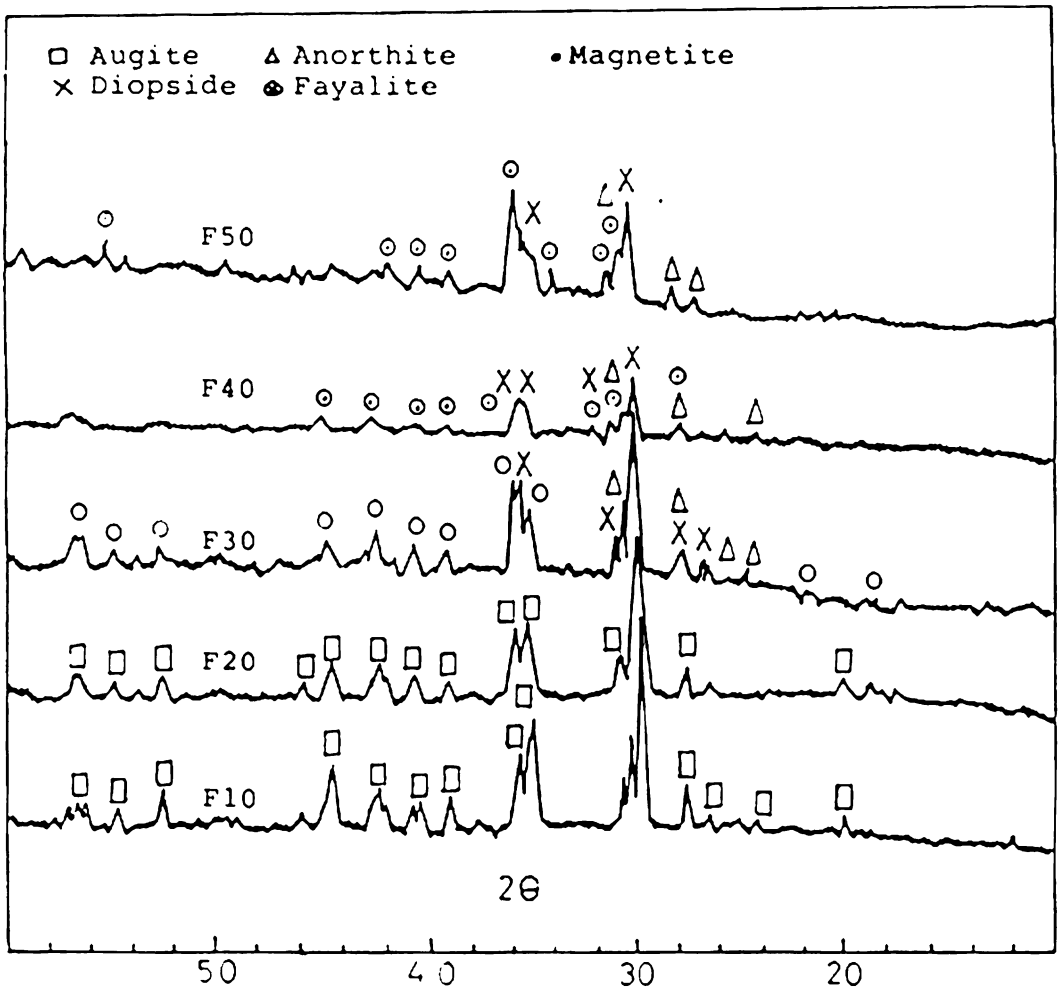

Fig. 12. X-ray diffraction patterns of glasses based on the fayalite–diopside–anorthite system heat-treated at 1000 °C for 2 h.

Al^{3+} ions may be responsible for encouraging bulk crystallization on going from F10 to F50 as a result of the possible change in its coordination from four to six. The coordination state of Al^{3+} ions in silicate glasses has been the subject of considerable debate. Physical property measurement on alkali silicate glasses [23,24] and alkaline earth silcate melts [25] suggested that Al_2O_3 acts amphoterically over a wide range of compositions i.e. aluminium can occur in both network forming and network modifying positions, and that Al^{3+} ions would, therefore, occur in both fourfold and sixfold coordination. These coordination states depend, to some extent, on the alkalinity or basicity of the silicate. Accordingly, in glasses with high alkaline earth silicate (Table 3) the Al ions, being in fourfold coordination, form $(AlO_4)^{5-}$ tetrahedra which enter the glass network and take part in the formation of a strong aluminium–silicon–oxygen framework; the formation of such closely packed tetrahedral structural groups diminishes the propensity towards devitrification [26]. This may explain why glass F10 has the highest content, 13.0 wt.% of Al_2O_3. Alkaline earth silicate (Table 3) is somewhat difficult to crystallize from (Fig. 12) the augite crystallized as the major phase in the samples with low fayalite (F10 and F20), although the calculated amount of diopside in these compositions constitutes only 46–52%. The formation of this augite pyroxene phase as the major phase may be due to the wide limits of isomorphous substitutions in the pyroxene formula. Thus, molecules $CaAl_2SiO_6$ can share in the building of the pyroxene structure with the aluminum ions occupying 4 and 6 coordination positions to form complex aluminous pyroxene solid solution.

F30 gives fayalite and anorthite with diopside. Further increase of the fayalite content to 40–50 wt.% (F40 and F50) and the fayalite disappeared and mangnetite appeared. The strong tendency of Al^{3+} to share the building of a complex pyroxene solid solution can be explained by the ability of Al^{3+} to take fourfold and sixfold coordination in crystalline silicates. The sharing of aluminium in these different structural positions is found to be controlled by the ratio between its ionic radius and the ionic radius of oxygen (0.43 Å), which is approaching the geometrical limits of stability between fourfold and sixfold coordinates (0.41 Å) [27].

The low activation energy of aluminous pyroxene (about 6 kcal/mol) compared with that of plagioclase (about 8–13 kcal/mol) [28] is one of the main factors which may favour the formation of pyroxene rather than plagioclase.

5. Conclusion

The present results showed different types of metallurgical slags that were experimented on as starting materials for making glass-ceramics. Silicon manganese slag and steel slag could be successfully used for making glass-ceramic materials. For making glass-ceramic materials with silicone manganese, the silicon manganese slag reached was about 90 wt.% and steel slag reached about 57 wt.% of the batch constituents. Depending on the composition, batches were melted in the range of 1200–1300 °C. It has been found that increasing the content of the bustamite phase in the glasses, results in an increased bulk crystallinity when treated at 1000 °C for 2 h. On the contrary, an increase in the content of the fayalite phase in the glasses results in decreased bulk crystallinity when treated at 1000 °C for 2 h.

References

[1] P.W. McMillan, Glass-Ceramic, 2nd Edition, Academic, New York, 1979.
[2] A.W.A. El-Shennawi, Crystallization in the System Spodumene–Willemite–Diopside, PhD thesis, Cairo University, 1977.
[3] G.H. Beall, Design of glass-ceramic, Rev. Solid State Science 3 (1989) 333.
[4] G. Partidge, An overview of glass-ceramic, part 1. Development and principal bulk application, Glass Technol. 35 (1994) 116.
[5] B. Locsei, in: Symposium on Nucleation and Crystallization in Glasses and Melts, Am. Ceram. Soc., Ohio, 1962, p. 71.
[6] L.A. Zhunina, V.N. Shara, V.F. Tsitko, N.N. Khrikova, The Structure of Glass, Consultant Bureau, New York, 1964.
[7] A.A. Omar, S.M. Salman, Crystallization of silicate glasses based on granite and dolomite mixtures, Cent. Glass-Ceram. Bull. 18 (1971) 32.
[8] G.A. Khater, The Use of Some Egyptian Clays the Production of Glass-Ceramic Materials, MSc thesis, Ain Shams University, 1986.
[9] G.A. Khater, The use of some Saudi Basalt for the production of glass-ceramic materials, Egyptian Minerologist (in press).
[10] A.W.A. El-Shennawi, M.A. Mandour, M.M. Morsi, S.A. Abdel-Hamed, Monopyroxene basalt based glass-ceramic, J. Am. Ceram. Soc. 82 (1999) 1181.
[11] G.H. Beal, H.L. Rittler, Basalt glass ceramic, Ceram. Bull. 5 (1976) 579.
[12] S. Carter, C.B. Ponton, R.D. Rawlings, Microstucture, chemistry, elastic properties and internal friction of silceram glass-ceramic, J. Mater. Sci. 23 (1988) 2622.
[13] M.D. Mashkovich, B.G. Varshall, Electrical properties of glass crystalline materials, Inorganic Material (USSR) (1967) 1454.
[14] A.W.A. El-Shennawi, The use of differential thermal analysis in the study of glass-ceramic, Ain Shams Sci. Bull. 24 (1983) 225.
[15] A.A. Omar, A.W.A. El-Shennawi, A.R. El-Ghennam, XV Conf. Silicate Industry and Silicate Science, Budapest, Hungary, 1989.
[16] S.D. Stookey, Catalzed crystallization of glass in theory and practice, Ind. Eng. Chem. 51 (1959) 805.
[17] W. Vogel, Inter-relationship between microheterogeneity, Glass Technol. 7 (1966).
[18] R. Roy, Metastable liquid immiscibility and subsolids nucleation, J. Am. Ceram. Soc. 43 (1960) 670.
[19] W. Hinz, P.O. Kinth, Phasentrennung and Keimbild ung bei der Herstellung von Vitrokeram, Glastech. Ber. 34 (1961) 431.
[20] W.B. Hillig, Symp. Nucleation and Crystallization in Glasses and Melts, Am. Ceram. Soc. Westerville, 1962.
[21] A.W.A. El-Shennawi, A.A. Omar, A.M. Morsy, Role of titania and titania-mixture in the nucleation and crystallization of spodumene–willemite–diopside glasses, Thermochem. Acta 58 (1982) 125.
[22] ASTM, Inorganic Index to the Powder File, ASTM Publication, 1979, Card No. 11-654.
[23] Y. Sakata, Unit cell dimension of synthetic aluminium diopside, Jap. J. Geol. George 28 (1957) 161.
[24] R.M. Douglas, The crystal structure of sanbronite, Am. Min. 43 (1985) 517.
[25] R.H. Rein, J. Chipman, Activities in the liquid solution SiO_2–CaO–MgO Al_2O_3 at 1600 °C, Trans AIME 233 (1965) 415.
[26] A.W.A. El-Shennawi, A.A. Omar, G.A. Khater, The crystallization of celsian polymorphs in some alkaline earth aluminosilicate glasses, Glass Technol. 32 (1991) 131.
[27] V.M. Goldschmiat, Geochemistry, Clarendon, Oxford, 1954.
[28] A.A. Omar, Influence of Isomorphous Substitution in Pyroxene on the Crystallization of Synthetic Basaltic Melts, PhD thesis, Moscow State University, 1965.